Nucleic Acids Research, 1996, Vol. 24, No. 19 **3693–3699**

Hydration of the RNA duplex r(CGCAAAUUUGCG)$_2$ determined by NMR

Maria R. Conte, Graeme L. Conn[1], Tom Brown[1] and Andrew N. Lane*

Division of Molecular Structure, National Institute for Medical Research, The Ridgeway, Mill Hill, London NW7 1AA, UK and [1]Department of Chemistry, University of Southampton, Southampton SO17 1BJ, UK

Received July 4, 1996; Revised and Accepted August 16, 1996

ABSTRACT

The so-called spine of hydration in the minor groove of AnTn tracts in DNA is thought to stabilise the structure, and kinetically bound water detected in the minor groove of such DNA species by NMR has been attributed to a narrow minor groove [Liepinsh, E., Leupin, W. and Otting, G. (1994) *Nucleic Acids Res.* 22, 2249–2254]. We report here an NMR study of hydration of an RNA dodecamer which has a wide, shallow minor groove. Complete assignments of exchangeable protons, and a large number of non-exchangeable protons in r(CGCAAAUUUGCG)$_2$ have been obtained. In addition, ribose C2′-OH resonances have been detected, which are probably involved in hydrogen bonds. Hydration at different sites in the dodecamer has been measured using ROESY and NOESY experiments at 11.75 and 14.1 T. Base protons in both the major and minor grooves are in contact with water, with effective correlation times for the interaction of ~0.5 ns, indicating weak hydration, in contrast to the hydration of adenine C2H in the homologous DNA sequence. NOEs to H1′ in the minor groove are consistent with hydration water present that is not observed in the analogous DNA sequence. Hydration kinetics in nucleic acids may be determined by chemical factors such as hydrogen-bonding more than by simple conformational factors such as groove width.

INTRODUCTION

Nucleic acids are strongly hydrated in both the crystal state and in solution and the degree of hydration determines the overall conformation. Hydration in DNA has been measured by a variety of methods including NMR (1–4), thermodynamics (5), and crystallography (6,7). Thus at low water activity, DNA adopts the A conformation, whereas at high water activity, it is found in the B conformation. In contrast, RNA is always in the A conformation. Chemically, the important difference between DNA and RNA is the 2′-OH on the sugar in RNA, though the methyl group of thymine affects primarily the thermodynamic stability of duplexes of either RNA or DNA (8).

Although there are numerous X-ray structures of DNA in both the B and A forms, there are no high resolution solution structures of DNA in the A form, and only a few solution structures of RNA. Many of the crystal structures have been reported on the hydration of DNA and RNA, and the results have been summarised in detail (9). In contrast, there have been only a few reports of hydration of nucleic acids using NMR (1–4,10) and none on RNA in solution.

The concentration of water is very high (~55 M), and therefore statistically can be expected to be close to all exposed sites on the surface of a solute particle. In the absence of any interaction between water and solute, the rate constant for dissociation of a water molecule from a solute surface depends on the diffusion constant, and can be expected to be ~$2–3 \times 10^9$ s^{-1} at 10°C (i.e. an average residence time of ~0.3–0.5 ns) (11). The diffusion limited association rate constant will be of similar magnitude, i.e. 10^9–10^{10} M^{-1} s^{-1}, so that the effective dissociation constant is ~0.2–2 M. The free energy change is comparable with the free energy of mixing, and represents the case where water is not thermodynamically bound. However, at 55 M water, the occupancy of each exposed site will be >96%. Thus, water can be considered to be bound if the effective correlation time is significantly longer than ~0.5 ns.

A particularly important structural role for water has been proposed in the spine of hydration found in the narrowed minor groove of dAnTn sequences (6,7) which has been proposed to be responsible for the relatively slow exchange of NMR-visible water molecules from the neighbourhood of the adenine C2H (1,2). Because an RNA duplex has a very wide, shallow minor groove, the groove-width hypothesis predicts that there should be no slowly exchanging water molecules in the minor groove. However, it is possible that other factors such as hydrogen bonding are important. Thus, the minor groove of RNA is lined with C2′-OH groups, and is therefore relatively more hydrophilic than the minor groove of DNA. It would therefore be expected that the minor groove of RNA should show extensive contact with water, particularly around the C2′ positions. We have therefore examined the hydration of r(CGCAAAUUUGCG)$_2$. The hydration properties of this molecule can be directly compared with the DNA analogue d(CGCAAATTTGCG)$_2$, which has been extensively studied by X-ray diffraction (12) and NMR methods (13).

MATERIALS AND METHODS

r(CGCAAAUUUGCG) was synthesised using phosphoramidite chemistry and purified by reversed-phase HPLC (14). A quantity of 112 A_{260} units of the purified and annealed dodecamer were

* To whom correspondence should be addressed

dissolved in 0.6 ml 90% H_2O:10% D_2O containing 0.01 M sodium phosphate, 100 mM KCl, 0.2 mM EDTA and 0.1 mM DSS, pH 7.

^1H NMR spectra were recorded at 14.1 T on a Varian Unity NMR spectrometer and at 11.75 T on a Varian UnityPlus spectrometer. 2D NMR spectra were recorded in the phase-sensitive mode (15). Spectra in H_2O were recorded using the Watergate pulsed gradient method for solvent suppression (16) with acquisition times of 0.4 s in t_2 and 0.05 s in t_1. NOESY spectra were obtained using mixing times of 25, 50, 100 and 250 ms. A ROESY spectrum was obtained with a mixing time of 25 ms, and a spin-lock field strength of 4.5 kHz.

NOESY spectra in D_2O were recorded at 30°C with acquisition times of 0.7 s in t_2 and 0.06 s in t_1, with mixing times of 50, 100 and 250 ms. A 2-quantum COSY experiment (17) was recorded with a mixing pulse of 135°, acquisition times of 0.5 s in t_2 and 0.04 s in t_1, with a 2-quantum creation time of 40 ms. In this experiment, cross-peaks are disposed either side of the two-quantum diagonal, which is free of peaks. Further, the 135° pulse suppresses the remote connectivities. The spectrum produced in this experiment was phased to pure absorption along F2, and absolute value along F1. Data matrices were transformed as 16384 by 2048 complex points, using a Gaussian function for apodisation in both dimensions.

Hydration was assessed by observing both NOEs and ROEs from water to different protons in cross-sections along F2 at the water frequency. In the absence of spin diffusion, ROEs are positive, and the cross-peaks have the opposite sign to the diagonal. Chemical exchange peaks in ROESY spectra are negative, and have the same sign as the diagonal. In NOESY spectra, exchange cross-peaks are negative, and in general, NOEs are also negative unless the effective correlation time is short (less than ~0.3 ns). The ratio of the cross-relaxation rate constants in the laboratory and rotating frames, R, depends only on correlation times and (known) Larmor frequencies. Thus, for a tightly bound water molecule (i.e. for which the residence time is longer than the rotational correlation time), the cross relaxation rate constants in the two experiments are given by:

$$\sigma_1 = a[6J(2\omega) - J(0)]/r^6 \quad \mathbf{1}$$

$$\sigma_r = a[3J(\omega) + 2J(0)]/r^6 \quad \mathbf{2}$$

$$R = [6J(2\omega) - J(0)]/[3J(\omega) + 2J(0)] \quad \mathbf{3}$$

where a is a nuclear constant and J(ω) are the spectral density functions.

Equation **3** predicts that the ratio R, will approach –0.5 for long correlation times, as in macromolecules. If the bound water molecule can undergo rapid, large amplitude motions, the spectral density functions become more complex. For sufficiently rapid internal motions, each spectral density function can be decomposed into two parts, corresponding to overall rotation of the complex, and internal mobility as (18):

$$J(\omega,\tau) = S^2J(\omega,\tau_0) + (1 - S^2)J(\omega,\tau_e) \quad \mathbf{4}$$

where S^2 is the order parameter, $\tau_e = \tau_0\tau_i/(\tau_0+\tau_i)$ and τ_0, τ_i are the correlation times for global rotation and internal motion, respectively. If the internal motion is of large amplitude, such that $S^2 = 0$, the form of the spectral density function reduces to that of a rigid rotor, except that it is determined by τ_e rather than τ_0. In this case, the value of R can vary between unity (very short correlation times) and –0.5 (long correlation times). This allows NOEs to become positive. An alternative is that water molecules are not strongly bound, but diffuse in and out of the molecular surface on a time-scale comparable with the global correlation time. Models of translation diffusion give quite complex spectral density functions (19), but the ratio, R, still depends only on the correlation time and Larmor frequency (and not on distances) (19–21). For this model, the correlation time is related to the diffusion coefficient of the diffusing water molecule, which may be smaller than that of pure water if there is an interaction between the water molecules and the solute particle. Hence, these models can provide limits on the effective correlation time for water-solute interactions as probed by NMR.

Experimentally, the ratio R was determined by measuring cross peak areas in cross-sections at the water frequency, and normalising them to the intensity of Cyt or Uri H5–H6 cross peaks. This eliminates the effects of autorelaxation and non-uniform excitation with the Watergate pulse. Corrections were made for off-resonance effects in the ROESY spectra as described (22,23). Effective correlation times were then determined using equation **3** for both rotational and translational diffusion models. Where absolute volume ratios were used, corrections were also made for the Watergate excitation profile, which is particularly important for the H1′ resonances.

Magnetisation time courses were calculated either analytically for three-spin systems, or by numerical integration of the appropriate Bloch equations for complete spin-systems, using the program NUCFIT (24). Coordinates were obtained for energy-minimised RNA using DISCOVER (Molecular Simulations, San Diego). Calculations were carried out assuming a correlation time of 5 ns and a recycle time of 3.5 s. The complete spin-system calculations also provided values for the autorelaxation rate constants of each proton.

RESULTS

NMR assignments

Non-exchangeable protons were assigned using a combination of NOESY and DQF-COSY and 2-quantum COSY in D_2O solution. Figure 1 shows a NOESY spectrum in D_2O recorded at 14.1 T and 30°C. It was possible to trace the sequential base–H1′–base proton connectivities. In addition, the adenine C2H resonances (and see below) showed three cross-peaks. The weak cross-peak corresponds to the intraresidue interaction with H1′, and the two strong peaks correspond to the sequential H2(i)–H1′(i+1) and the cross-strand H2(i)–H1–(i–1) interactions. The latter cross-peak was more intense than expected for standard A-RNA, where this distance is ~4.5 Å, compared with the sequential H2–H1′ distance of ~3.6 Å. The H2′ resonances were assigned using the strong H1′–H2′ NOE cross-peaks, and also the sequential pathways H1′(i)–H2′(i)–H8/H6(i+1) pathway. H3′ peaks were assigned from both the NOESY, using the intraresidue H8/6(i)–H′(i) and sequential H3′(i)–H8/H6(i+1) cross-peaks, and the H2′–H3′ cross-peaks in the DQF-COSY and DQ-COSY spectra (not shown). The H4′ resonances were initially assigned from traces through H1′ of NOESY spectra. The most intense peak in this cross-section is the H2′, followed by the H4′ and H3′ peaks. The H4′ resonance was assigned by elimination, and by H3′–H4′ cross-peaks in the DQF-COSY spectrum. The H3′ and H4′ resonances were confirmed using the 2-quantum COSY experiment, which revealed scalar interactions between protons of similar chemical shifts (not shown). The 2Q-COSY and DQF-COSY spectra also revealed numerous cross-peaks that

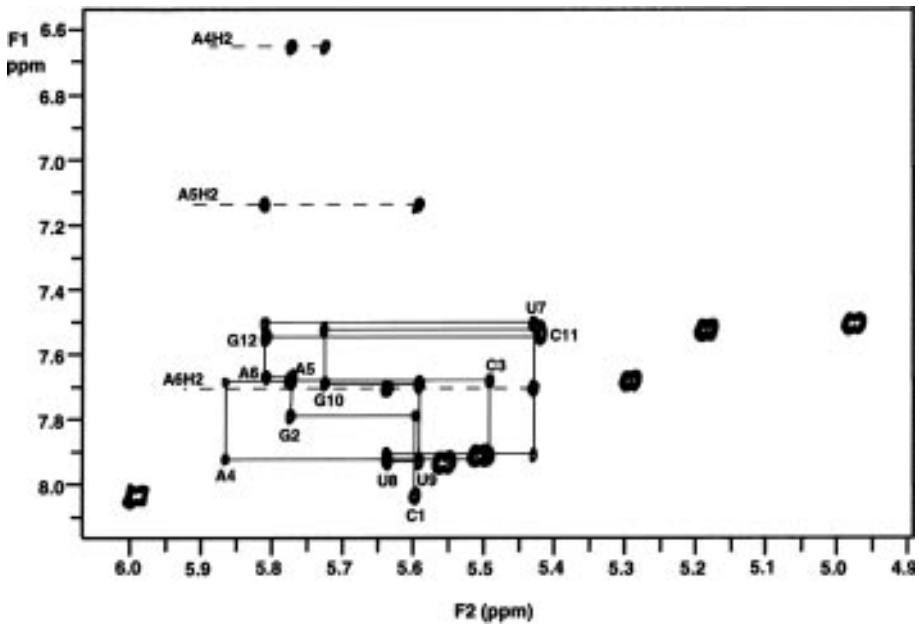

Figure 1. NOESY spectrum of r(CGCAAAUUUGCG)$_2$ in D_2O. The spectrum was recorded at 30°C, 14.1T as described in Materials and Methods, with a mixing time of 250 ms.

could arise only from inequivalent H5′/H5″, which in many instances had large differences in chemical shifts. In some instances, these could be independently verified from NOESY spectra by observing H6–H5/H5″ and H1′–H5′/H5″ (cf. U7 and C11). The assignments are given in Table 1.

Figure 2A shows a NOESY spectrum recorded in H_2O at 10°C and 14.1 T. The two-fold symmetry of the duplex was confirmed by the observation of six resonances in the 12–14 p.p.m. region of the spectrum. The broadest resonance at 12.47 p.p.m. was assigned to the terminal G12N1H. The remaining imino protons were assigned from the NOE between neighbouring imino protons, and in the case of UN3H, by strong NOEs to the base-paired AC2H, which were independently assigned from NOEs to H1′ in the D_2O NOESY spectra.

Cytosine amino protons were assigned according to the strong NOE between the hydrogen bonded amino proton and the N1H of the base-paired G. The non-H-bonded amino proton was then found from the strong NOE within the NH_2 group. These assignments were further verified by the strong NOE from the upfield amino proton to the H5 of the same nucleotide, and the weaker NOE to the downfield amino proton.

Table 1. ^{1}H assignments in r(CGCAAAUUUGCG)$_2$

Base	H8/6	H5/Me H2	H1′	H2′	H3′	H4′	NH	NH_2
C1	8.04	5.99	5.60	4.52	4.56	4.34	–	8.18, 7.00
G2	7.80	–	5.77	4.57	4.69	(4.50)	13.08	n.d.
C3	7.69	5.29	5.49	4.52	(4.56)	(4.44)	–	8.39, 6.79
A4	7.93	6.67	5.87	4.58	4.73	4.50	–	7.71, 6.35
A5	7.69	7.15	5.77	4.52	4.64	(4.50)	–	7.80, 6.75
A6	7.68	7.72	5.81	4.42	4.50	nd	–	7.96, 6.77
U7	7.52	4.97	5.43	4.34	4.38	(4.42)	13.98	–
U8	7.92	5.51	5.64	4.41	4.48	nd	13.77	–
U9	7.95	5.56	5.59	4.52	4.54	4.46	13.12	–
G10	7.70	–	5.73	4.42	4.57	4.52	12.44	7.95, 5.80
C11	7.54	5.19	5.42	4.26	4.42	4.34		8.31,6.75
G12	7.56	–	5.81	4.08	4.26	4.19	12.88	n.d.

C1 (5′,5″ 3.94,4.04) p.p.m.; C2′-OH 6.7, 6.9 p.p.m. Proton assignments are given for 30°C, except for exchangeable protons which are given for 10°C. Shifts in parentheses are tentative. n.d., not determined.

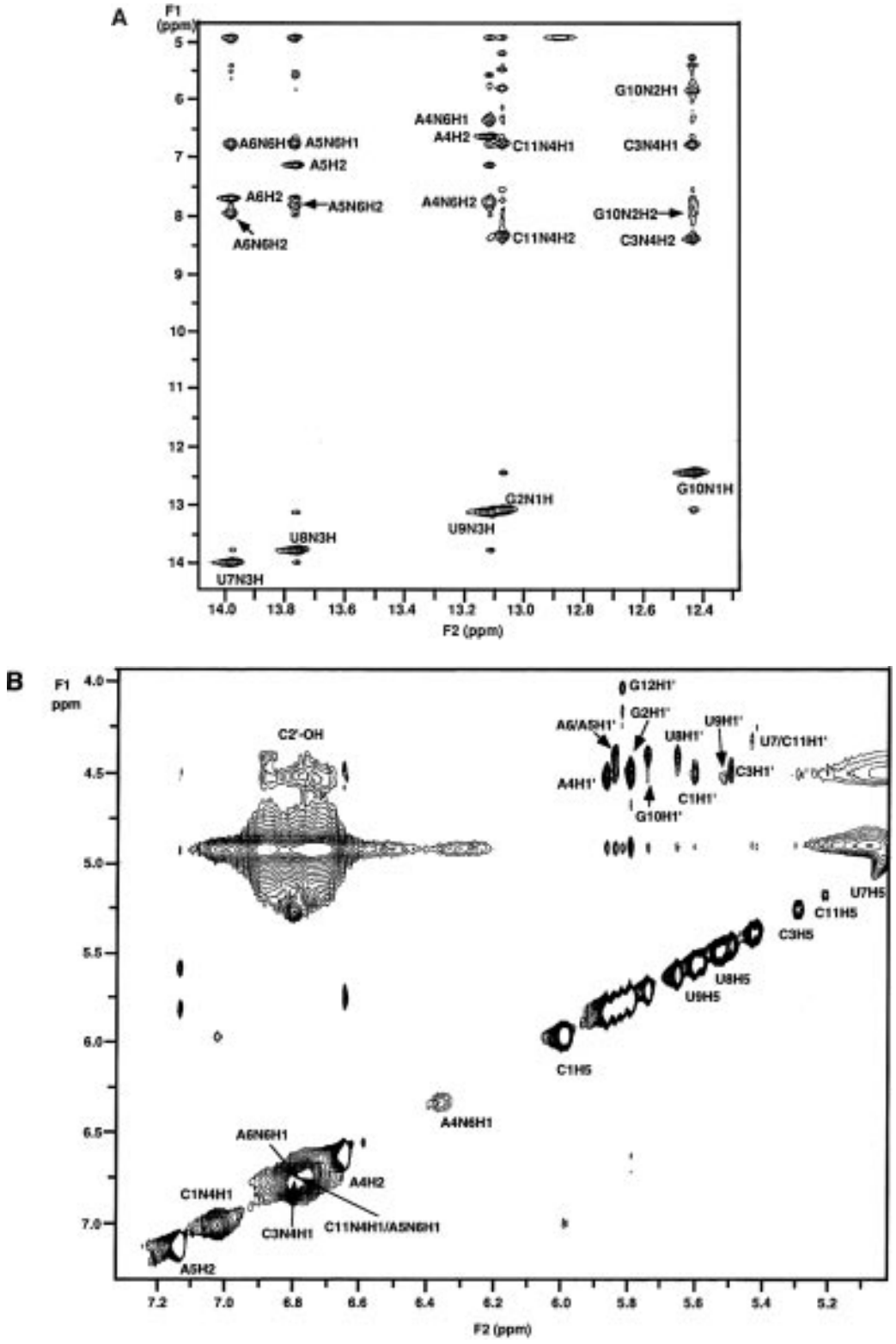

Figure 2. NOESY spectrum of r(CGCAAAUUUGCG)$_2$ in H_2O. The spectrum was recorded at 10°C as described in the Materials and Methods. (**A**) Imino and amino protons (mixing time = 250 ms, 14.1 T). (**B**) Hydroxyl protons (mixing time = 50 ms, 11.75 T).

Medium strength NOEs were also observed between pairs of exchangeable protons ($\delta \approx 8$ and 6.7) with UN3H. These resonances also showed a very intense mutual NOE, and can be identified as the N6 amino protons of the base-paired adenines. The ANH_2 were then assigned using the method described for the cytosine amino protons (see above). The amino protons of G10

were found in a similar manner, but the amino protons of G2 and G12 were not assigned. The assignments of the exchangeable protons are collected in Table 1.

As Table 1 and Figure 2B show, the non-hydrogen-bonded amino protons resonate between 6.3 and 7 p.p.m. In the 1D spectrum, there were two intense peaks at 6.75 and 6.85 p.p.m. The former contains the amino protons of A5, A6, C3 and C11, and the latter no amino protons. Hence, these two peaks should account for only four protons. However, the integral of the two peaks was at least 10 protons, which indicates that there must be at least another six exchangeable protons in this region. The only remaining candidate amino protons are from G2 and G12. Models of A-RNA showed that there are no amino protons within 5 Å of H2′ or H3′ within nucleotides in the A conformation and the closest amino proton is the non H-bonded N6H2 of G to the neighbouring cross-strand H2′ of the preceding residue, which is ~4.3 Å. The NOE calculated for the A-RNA structure, excluding chemical exchange of the amino proton with water, was very small. Also, in the DNA analogue of this sequence, there were no protons that exchange with water under similar conditions (Lane, Frenkiel and Jenkins, unpublished data). However, the C2′-OH is close to the C2′-H, and NOE cross-peaks were observed between the resonances near 6.85 p.p.m. and peaks at 4.3–4.5 p.p.m. (Fig. 2B), which correspond to H2′ and H3′ (Table 1). Further, it has been reported that the C2′-OH in RNA resonates at ~ 6.7 p.p.m. (25), and between 6.1 and 6.9 p.p.m. in simple carbohydrates, where they can be observed only at low temperatures (26). We conclude that the additional intensity near 6.7–6.8 p.p.m. arises from at least six C2′-OH. However, the resolution of the spectrum in this region and in the C2′-H region prevented us making firm sequence-specific assignments. Nevertheless, it is clear that the RNA OH exchange quite slowly under the conditions of these experiments, suggesting that these proton are involved in H-bonding interactions, such as to the nearby O3′ or to the O4′ of the next sugar (25,27–29).

Hydration

Figure 3 shows cross-sections at the water frequency from NOESY and ROESY spectra of r(CGCAAAUUUGCG)$_2$ recorded at 10°C and 14.1 T, using mixing times of 50 and 25 ms, respectively. Imino protons, which resonate between 12 and 14 p.p.m. (not shown) showed some exchange with water, in the order: G12N1H>U7N3H≈U8N3H>U9N3H≈G2N1H>G10N1H(≈0). The N4H2 (hydrogen bonded amino proton) of C3 and C11 showed essentially no exchange whereas that of C1 exchanged extensively with the water. The intense peaks between 6.6 and 6.9 p.p.m. arise from chemical exchange primarily of C2′-OH (see above) with water. The relatively strong peak at 7.58 p.p.m. is predominantly a direct NOE between U7H5 (δ = 4.97 p.p.m.) and U7H6 (cf. Table 1). However, it provides a useful internal intensity standard, as the distance between these protons is 2.42 Å.

The degree of hydration at different non-exchangeable protons was assessed from the sign and magnitude of water-solute NOE in cross-sections at the water frequency as described in Materials and Methods. Values of R for each resolved resonance are given in Table 2. At 14.1 T, some of the H8/H6 showed negative NOEs and positive ROEs (Fig. 3). In general the absolute values of R are smaller at 11.7 T than at 14.1 T, which is characteristic of correlation times close to 0.5 ns. These kinds of NOEs are similar to those found in DNA duplexes (1–4). The adenine C2H-water

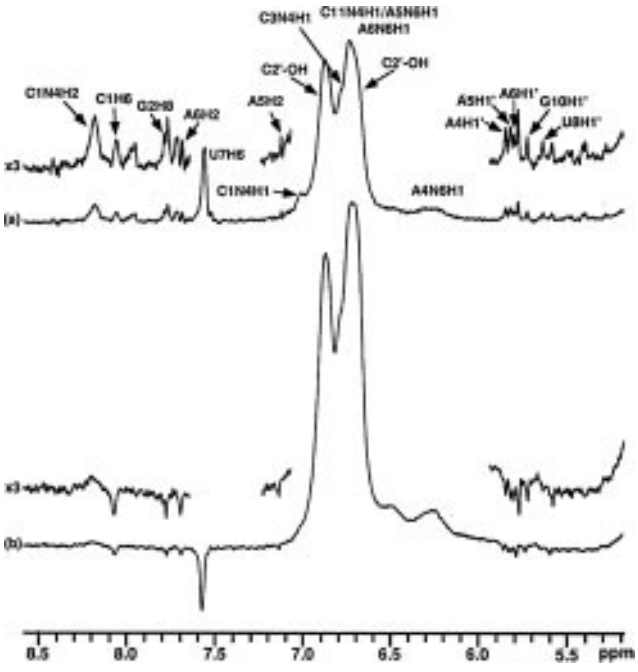

Figure 3. Cross-sections at the water frequency in NOESY and ROESY spectra of r(CGCAAAUUUGCG)$_2$. Upper trace NOESY (50 ms mixing time), lower trace ROESY (25 ms mixing time). The large peak at 7.58 p.p.m. arises from cross-relaxation of U7H6 with U7H5 (δ = 4.98 p.p.m.).

NOE cross-peaks were also very small indicating a short correlation time near 0.5 ns. The normalised cross-peak intensities in the NOESY spectrum (~0.06 at 600 MHz), and R values were quite small for these peaks compared with those of the analogous DNA duplex (Lane, Frenkiel and Jenkins, unpublished). The upper limit to correlation time for the water–C2H vector is equal to that for overall rotation of the molecule (i.e. when the water is irrotationally bound). For this case, as the observed NOE was 0.06 as intense as that of the cytosine H6–H5 NOE, we can calculate an upper limit to the water C2H distance of as NOE(water–C2H)/NOE(CytH6–H5)≈[(r(H6–H5)/r(water–C2H)]^6 for a short mixing time, assuming r(H6–H5) = 2.42 Å. However, under these conditions, the NOE would be independent of the magnetic field strength, in contradiction with the results (Table 2). Hence, the effective correlation time must be short, and which requires a distance shorter than 3.8 Å. The small effective correlation times for both AC2H and H8/H6 are consistent with rapid, large-scale internal motion of the water or a short residence time (or both). In either interpretation, these water molecules can be considered to be at most very weakly bound. This indicates that in RNA, both the major groove, and at least some aspects of the minor groove, are weakly hydrated. This is in contrast with the DNA analogue, where the minor groove is relatively strongly hydrated in the AnTn tract, as observed also by others for different sequences (1–4).

Cross-peaks to the H1′ resonances were observed, which are not usually seen in DNA except at the ends of the duplex or at much longer mixing times (3). Note that the resonances between 5.5 and 6 p.p.m. are significantly attenuated by the Watergate pulse, and so appear less intense than they should. In principle, these latter NOE peaks could arise via several mechanisms. First

there could be a water molecule with a long residence time close to H1′. Second there could be an NOE between the C2′-OH and the C1′-H with rapid exchange between the C2′-OH and water protons. Both mechanisms would give rise to a negative NOE and positive ROE. Other mechanisms involving two sequential NOE transfers from water to C2′-OH to C1′-H would give rise to a negative ROE, in contrast to the observations (Fig. 3 and Table 2). There are also no H2′ that coresonate with the water that could give rise to a direct NOE (Table 1). We have assigned at least six C2′-OH protons to the peaks at 6.7 and 6.85 p.p.m. (see above), which are therefore in slow exchange with water on the chemical shift time scale. It has been reported that the exchange rate of the secondary alcohol proton should be around 10–20 s^{-1} in RNA at 10°C (25). However, because there were only very weak NOEs from the hydroxyl protons to H1′ at a mixing time of 50 ms, and no detectable NOE at 25 ms (Fig. 2), most of the magnetisation transfer from water to H1′ cannot be via the route $H_2O \rightarrow$C2′-OH$\rightarrow$H1′. We have calculated the magnitude of the exchange mediated NOE for different geometries. The OH protons can in principle be in Van der Waals contact with H1′, which would give rise to an extremely intense OH–H1′ NOE (and also the exchange mediated NOE from water), which was not observed. For an exchange rate constant up to at least 150 s^{-1}, calculations (not shown) indicate that the normalised water–H1′ NOE for this mechanism should increase markedly with increasing mixing time, whereas the observed NOE was essentially independent of the mixing time. Only if the exchange rate constant is very large (when the OH peak merges with the solvent peak) does the lag in the NOE build up curve become undetectable. In this case, the observed magnetisation transfer from water to H1′ depends exclusively on the cross-relaxation rate constant C2′OH–H1′. Indeed, the small observed NOE indicates that the C2′-OH must be pointing away from the H1′. Most significantly, whereas there are signifcant cross-peaks between H1′ and water, there are no cross-peaks of comparable or greater intensity between the C2′-OH and the H1′, as would be required for the exchange mediated pathway.

Table 2. Effective water–r(CGCAAAUUUGCG)$_2$ correlation times

	R		τ_{eff}/ns
	14.1 T	11.75 T	
G2H8	<0	≈0	0.3–0.8
G10H8	<0	≈0	0.3–0.8
A5H2	–0.2	≈0	0.3–0.8
A6H2	–0.3	–0.13	0.6–1
A4H1′	–0.5	–0.38	>0.5[a]
A5H1′	–0.47	[b]	>0.5[a]
A6H1′	–0.44	[b]	>0.5[a]
U8H1′	–0.5	[c]	>0.5[a]
G10H1′	–0.42	–0.28	>0.5[a]

[a]See text.
[b]Peaks overlap at 500 MHz.
[c]Peak too small to quantitate.
R is the ratio of the cross-relaxation rate constant in the laboratory frame to that in the rotating frame. τ_{eff} is the effective correlation time. R was determined at 10°C as described in Materials and Methods.

To reduce the contribution from exchange further, we have recorded a NOESY spectrum at 5°C with a mixing time of 30 ms. At the lower temperature, cross-relaxation rates should increase by ~17%, and decrease the OH exchange rate by a factor of ~2. Comparison of the intensity of the peaks with and without presaturation showed a reduction of ~60%, indicating an exchange rate constant of similar magnitude to the spin-lattice relaxation rate constant. As the latter is <10 s^{-1}, the exchange rate constant should also be < 10 s^{-1}. Water–H1′ cross-peaks were again present, and of an intensity ~30–40% of the U7 H5–H6 cross-peak intensity.

It is notable that whereas there were NOEs between the C2′-OH and C2′-H for most if not all nucleotides, there was no such NOE for the well-resolved G12, for which there is no 3′-phosphate or possible 3′ nucleotides to protect this terminal OH, which is not visible under these conditions. Hydrogen bonding of the (NMR visible) hydroxyl protons would place them ~3.4 Å from H1′, and give rise to a very small direct NOE, and therefore a very much smaller exchange mediated NOE. This suggests that a significant fraction of the observed transfer of magnetisation from water to H1′ in this RNA molecule is direct. As the observed NOE was negative, the effective correlation time for the water–H1′ interaction must be longer than ~0.5 ns (Table 1).

DISCUSSION

We have shown that C2′-OH can be observed in RNA under appropriate conditions, and that they are probably hydrogen bonded to groups within the RNA molecule. This indicates that additional information is available about RNA conformation and stability. Measurements of the NOEs involving the ribose hydroxyl protons should assist in the calculation of structures.

Both grooves of the RNA are clearly in contact with water, as has been observed by NMR for DNA. RNA has a deep major groove and a wide, shallow minor groove. Further, in RNA, the minor groove should be quite hydrophilic owing to the presence of the C2′-OH groups. However, the presence of water molecules close to H1′ occurs despite the wide and shallow minor groove of RNA. This is in contrast to the DNA analogue, d(CGCAAATTTGCG)$_2$, which is the B form and has a narrow minor groove in the A3T3 tract (12,13). Slowly exchanging water molecules have been detected in the minor groove in the region of the adenine residues of the related d(CGCGAATTCGCG)$_2$, and more rapidly exchanging water elsewhere (2,3). In DNA there is no nearby hydroxyl group to stabilise a water molecule, and under conditions similar to those used in this work, no NOEs were observed between water and H1′ (Lane, Jenkins and Frenkiel, unpublished). Because the hydroxyl proton exchanges with the solvent, it must be both accessible to, and interact with water, which indicates hydration at this site. Our results indicate that it is possible for water protons to be sufficiently close to H1′ for a direct NOE to be observed, and that hydrogen bonding to the hydroxyl oxygen may be responsible for the relatively long residence time, compared with DNA. This would be consistent with recent X-ray studies of RNA duplexes where water molecules interacting directly with the C2′-OH have been observed (27–29).

The reason for slow exchange in dAnTn tracts may be related more to the high propeller twist in these sequences, rather than the narrowed minor groove *per se*, which allows bridging of water molecules between neighbouring base pairs. This interaction is not possible in mixed-sequence DNA or RNA, where as we have shown the AdeC2H is only weakly hydrated. However, even in the narrowed minor groove of AnTn DNA tracts, hydration near to H1′ is very weak or non-existent, whereas in RNA it is substantial, and can be attributed to the presence of the OH group. The water close to this group is relatively long lived, which does

not correlate with a narrow minor groove. Although only a lower limit to the water residence time can be obtained by NMR, we imagine that even the long-lived molecules have residence times in nanoseconds rather than much longer as is sometimes observed in proteins (20). This is supported by the observed dependence of the ratio R on the magnetic field strength. For correlation times longer than ~2 ns, R becomes independent of the magnetic field strength, whereas we observed a significant magnetic field dependence for all protons (Table 2).

ACKNOWLEDGEMENTS

This work was supported by the Medical Research Council of the UK, by a Wellcome Travelling Research Fellowship to MRC and a Royal Society of Edinburgh Caledonian Research Fellowship to GC. We thank Dr J. Feeney for helpful discussions.

REFERENCES

1 Liepinsh, E., Otting, G. and Wüthrich, K. (1992) *Nucleic Acids Res.* **20,** 6549–6553.
2 Liepinsh, E., Leupin, W. and Otting, G. (1994) *Nucleic Acids Res.* **22,** 2249–2254.
3 Kubinec, M.G. and Wemmer, D.E. (1992) *J. Am. Chem. Soc.* **114,** 8739–8740.
4 Fawthrop, S.A., Yang, Ji-Chun and Fisher, J. (1993) *Nucleic Acids Res.* **21,** 4860–4866.
5 Chalikian, T.V., Plum, G.E., Sarvazyan, A.P. and Breslauer, K.J. (1994) *Biochemistry* **33,** 8629–8640.
6 Drew, H.R. and Dickerson, R.E. (1981) *J. Mol. Biol.* **151,** 535.
7 Privé, G.G., Heinemann, U., Chandrasegaran, S., Kan, L-S., Kopka, M.L. and Dickerson, R.E. (1987) *Science* **238,** 498–504.
8 Wang, S. and Kool, E.T. (1995) *Biochemistry* **32,** 4125–4132.
9 Berman, H.M. (1994) *Curr. Opin. Struct. Biol.* **4,** 345–350.
10 Radhakrishnan, I. and Patel, D.J. (1994) *Structure* **2,** 395–405.
11 Amdur, I. and Hammes, G.G. (1966) *Chemical Kinetics: Principles and Selected Topics.* Chapter 2. McGraw Hill, New York, USA.
12 Edwards, K.J., Brown, D.G., Spink, N., Skelly, J.V. and Neidle, S. (1992) *J. Mol. Biol.* **226,** 1161–1173.
13 Jenkins, T.C., Brown, D.G., Neidle, S. and Lane, A.N. (1993) *Eur. J. Biochem.* **213,** 1175–1184.
14 Ebel, S., Brown, T. and Lane, A.N. (1994) *Eur. J. Biochem.* **220,** 703–715.
15 States, D.J., Haberkorn, R.A. and Ruben, D.J. (1982) *J. Magn. Reson.* **48,** 286–292.
16 Piotto, M., Saudek, V. and Sklenar, V. (1992) *J. Biomol. Str.* **2,** 661–665.
17 Mareci, T.H. and Freeman, R. (1983) *J. Magn. Reson.* **51,** 531–535.
18 Lipari, G. and Szabo, A. (1982) *J. Am. Chem. Soc.* **104,** 4559–4570.
19 Ayant, Y., Belorizky, E., Fries, P. and Rosset, J. (1977) *J. Phys. (Paris)* **38,** 325–337.
20 Abragam, A. (1965) *Principles of Nuclear Magnetism.* Ch. VIII. Oxford University Press, Oxford, UK.
21 Otting, G., Liepinsh, E. and Wüthrich, K. (1991) *Science* **254,** 974–980.
22 Griesinger, C. and Ernst, R.R. (1987) *J. Magn. Reson.* **75,** 261–271.
23 Leeflang, B.R. and Kroon-Batenburg, L.M.J. (1992) *J. Biomol. NMR* **2,** 495–518.
24 Lane, A.N. (1990) *Biochim. Biophys. Acta* **1049,** 189–204.
25 Leroy, J-L., Broseta, D. and Guéron, M. (1985) *J. Mol. Biol.* **184,** 165–178.
26 Poppe, L. and van Halbeek, H. (1994) *Nature Struct. Biol.* **1,** 215–216.
27 Leonard, G.A., McAuley-Hecht, K.E., Ebel, S., Lough, D.M., Brown, T. and Hunter, W.N. (1994) *Structure* **2,** 483–494.
28 Egli, M., Portmann, S. and Usman, N. (1996) *Biochemistry* **35,** 8489–8484.
29 Wahl, M.C., Ban, C., Sekharudu, C., Ramakrishnan, B. and Sundaralingam, M. (1996) *Acta Cryst.* **D52,** 655–667.